

## STUDIES

SPECIAL ISSUE: THE ROLE OF SEED DISPERSAL IN PLANT POPULATIONS:  
PERSPECTIVES AND ADVANCES IN A CHANGING WORLD

## Individual variation in dispersal and fecundity increases rates of spatial spread

Sebastian J. Schreiber<sup>1,\*</sup> and Noelle G. Beckman<sup>2</sup><sup>1</sup>Department of Evolution and Ecology and Center for Population Biology, University of California, Davis, CA 95616, USA,<sup>2</sup>Department of Biology and Ecology Center, Utah State University, Logan, UT 84322, USA\*Corresponding author's email address: [sschreiber@ucdavis.edu](mailto:sschreiber@ucdavis.edu)

Associate Editor: Haldre Rogers

Citation: Schreiber SJ, Beckman NG. 2020. Individual variation in dispersal and fecundity increases rates of spatial spread. AoB PLANTS 12: plaa001; doi: 10.1093/aobpla/plaa001

## Abstract

Dispersal and fecundity are two fundamental traits underlying the spread of populations. Using integral difference equation models, we examine how individual variation in these fundamental traits and the heritability of these traits influence rates of spatial spread of populations along a one-dimensional transect. Using a mixture of analytic and numerical methods, we show that individual variation in dispersal rates increases spread rates and the more heritable this variation, the greater the increase. In contrast, individual variation in lifetime fecundity only increases spread rates when some of this variation is heritable. The highest increases in spread rates occur when variation in dispersal positively co-varies with fecundity. Our results highlight the importance of estimating individual variation in dispersal rates, dispersal syndromes in which fecundity and dispersal co-vary positively and heritability of these traits to predict population rates of spatial spread.

**Keywords:** Dispersal; individual variation; integrodifference equations; range expansion; speed of invasion; trait evolution.

## Introduction

Predicting the spatial spread of species over time is a central question in ecology (Hastings *et al.* 2005; Jongejans *et al.* 2008). Mathematical models combining demography and dispersal have a long history of providing insights about the ecology and evolution of spatial spread (Skellam 1951; Kot *et al.* 1996; Hastings *et al.* 2005; Beckman *et al.* 2020). These models have guided conservation and management decisions to control the spread of invasive species (e.g. Shea *et al.* 2010) and are used to make predictions about the persistence of species under shifting climates (e.g. Travis *et al.* 2011; Santini *et al.* 2016). Traditionally, these models relied on mean estimates of dispersal and demographic rates. These rates, however, often exhibit substantial individual variation within populations

(reviewed in Schupp *et al.* 2019). As this individual variation is known to have important consequences for many ecological and evolutionary processes (Bolnick *et al.* 2011; Moran *et al.* 2016; Snell *et al.* 2019), it is natural to ask what effect do they have on rates of spatial spread.

In plants, variation in dispersal rates arises from intrinsic variation in trait expression among and within individuals and extrinsic variation based on the environmental context of the plant (Schupp *et al.* 2019; Saastamoinen *et al.* 2018). Saastamoinen *et al.* (2018) found that while plants can have high levels of heritability in dispersal traits, there can be a wide range of heritability that depends on the specific trait measured and the environment in which it was measured. Theoretical

Received: 12 July 2019; Editorial decision: 27 September 2019; Accepted: 8 May 2020

© The Author(s) 2020. Published by Oxford University Press on behalf of the Annals of Botany Company.

This is an Open Access article distributed under the terms of the Creative Commons Attribution License (<http://creativecommons.org/licenses/by/4.0/>), which permits unrestricted reuse, distribution, and reproduction in any medium, provided the original work is properly cited.

studies have studied the effects of non-heritable and heritable variation in dispersal rates on spatial spread. Petrovskii and Morozov (2008) and Stover *et al.* (2014) found that non-heritable variation in dispersal rates, such as due to phenotypic plasticity in response to local environmental heterogeneity (Johnson *et al.* 2019), leads to fatter dispersal kernels and faster rates of spatial spread. Alternatively, theoretical studies accounting for only heritable variation found selection for increased dispersal rates on the edges of a species' range resulting in accelerating rates of spatial spread (Travis and Dytham 2002; Hughes *et al.* 2007; Phillips *et al.* 2008, 2010; Travis *et al.* 2009; Bouin *et al.* 2012; Perkins *et al.* 2013). Empirical studies of expanding plant populations have supported some of these theoretical predictions (Cwynar and MacDonald 1987; Huang *et al.* 2015; Williams *et al.* 2016a; Tabassum and Leishman 2018, 2019). However, we still lack a full understanding of the relative contributions of heritable and non-heritable variation in dispersal rates on spread rates, and whether co-variation among individuals in dispersal and demographic rates facilitates or constrains spread rates.

Rates of spatial spread are likely to depend on the co-variance of dispersal with other traits under selection (Saastamoinen *et al.* 2018). Within populations, higher fecundity in plants is expected to increase the distance seeds are dispersed (Clark *et al.* 1998a; Norghauer *et al.* 2011). The number of fruit produced varies substantially among individuals within and across years in natural systems (e.g. Norghauer *et al.* 2011; Norghauer and Newbery 2015) with moderate to high heritability found in crop systems (e.g. Jindal *et al.* 2010; Usman *et al.* 2014). More generally, dispersal and life-history traits may co-vary to produce integrated strategies known as dispersal syndromes (Ronce and Clobert 2012) or dispersal may vary independently from other life-history traits (Bonte and Dahirel 2017). Dispersal syndromes may arise due to a variety of proximate and ultimate causes (reviewed in Ronce and Clobert 2012), including trade-offs in allocation, similar responses in expression to environmental conditions, genetic correlations among traits, joint selection on several traits or selection on dispersal constrained by or constraining the evolution of other traits. Across species, Beckman *et al.* (2018) found species with fast life-history strategies dispersed their seeds further than species with slow life-history strategies. Within species, dispersal is predicted to be an independent axis of other life-history traits (Bonte and Dahirel 2017), although this is not well-studied in plants.

To better understand the simultaneous effects of heritable and non-heritable co-variation in dispersal and demographic rates on spatial spread, we introduce a new class of integral difference equation models. These spatially explicit models simultaneously account for individual variation in lifetime fecundities and dispersal rates. This variation is allowed to be discrete or continuous, and heritable or non-heritable. Using this model, we explore the effects of variation in dispersal and demographic rates among individuals on the spread rate of populations, by first considering the separate effects of variation in dispersal and fecundity varying among individuals and then the joint effect of dispersal and fecundity co-varying among individuals. Our mathematical analysis, buttressed by numerical simulations, highlights that individual variation in dispersal rates, generally, increases rates of spatial spread, while non-heritable variation in fecundity has no effect. In contrast, when individual variation in fecundity co-varies positively with dispersal rates, it increases spread rates. Furthermore, heritability of either form of variation always increases spread rates.

## Model and Methods

Our models consider a population of plants living along a one-dimensional transect. Individuals vary in their production of seeds and the mean distance that a seed disperses. We consider two forms of the model: one with random transmission of individual traits and another allowing for non-random transmission of the traits. Both forms of the models are integrodifference equations that have been used extensively to model spatial spread (Kot *et al.* 1996; Neubert and Caswell 2000). For the model with non-random transmission, the population is structured by the trait in every spatial location. The changes in this local population structure are determined by a matrix model for discretely structured traits and by an integral projection model for continuously structured traits. For both types of models, we use the methods of Ellner and Schreiber (2012) to identify the asymptotic rates of spatial spread. Using these methods, we develop explicit formulas for how both forms of individual variation alter spatial rates of spread. As these formulas are derived in the limit of small individual variation, we also numerically investigate an empirically based model to demonstrate that the insights from our formulas apply to larger amounts of individual variation.

### Models with random transmission

Let  $n_t(x)$  denote the population density at location  $x$  in generation  $t$ . Under low-density conditions, individual plants produce  $f$  seeds during their lifetime. Each of these seeds disperses, on average, a distance of  $\ell$  m. We call this mean dispersal distance, the dispersal rate (i.e. the average number of metres a seed moves in a generation). The density of individuals with these characteristics equals  $\rho(f, \ell)$ . For seeds with a dispersal rate of 1 m, let  $k_1(v)dv$  be the infinitesimal probability that these seeds disperse from location  $x$  to location  $x + v$ . We assume that the dispersal kernel for a group of seeds with dispersal rate  $\ell$  equals  $k_\ell(v) = k_1(v/\ell)/\ell$ , i.e. the shape of the dispersal kernel is common to all seeds. The density of individuals with dispersal rate  $\ell$  equals  $\rho_\ell(\ell) = \int \rho(f, \ell) df$ . The population-level dispersal kernel corresponds to averaging dispersal kernels  $k_\ell$  across this individual variation (Fig. 1):

$$k_{\text{pop}}(v) = \int k_\ell(v) \rho_\ell(\ell) d\ell.$$

Petrovskii and Morozov (2008) call this population-level kernel a statistically structured dispersal model.

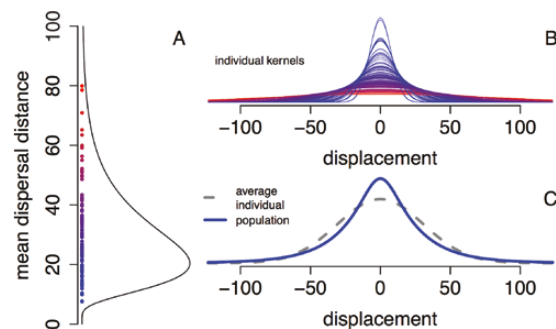


Figure 1. Individual variation in dispersal rates and the population-level dispersal kernel. In (A), variation among 100 maternal trees in their seed dispersal rates (mean dispersal distance). In (B), the Gaussian dispersal kernels of the 100 individuals from (A). In (C), the population-level dispersal kernel (i.e. the average of the kernels from (A)) in solid blue and the dispersal kernel of individuals with the average dispersal rate in dashed grey.

If  $D(n_t(y))$  corresponds to a density-dependent reduction in lifetime fecundity at location  $y$ , then the spatial dynamics of the population is

$$n_{t+1}(x) = \int_{-\infty}^{\infty} \left( \iint k_{\ell}(x-y) f \rho(f, \ell) df d\ell \right) D(n_t(y)) n_t(y) dy. \quad (1)$$

Without loss of generality, we assume that  $D(0) = 1$ . Furthermore, we assume that  $D(n) \leq D(0)$  for all densities  $n \geq 0$ , i.e. the lifetime fecundity of an individual is maximal at low densities. This assumption allows us to use the linearization principle for computing invasion speeds (Kot et al. 1996; Neubert and Caswell 2000; Ellner and Schreiber 2012).

While we have presented our model in equation (1) for continuously structured traits, one can write a similar model for discretely structured traits by replacing the double integral  $\iint$  with a double sum  $\sum_i \sum_j$  and replacing the infinitesimal probabilities  $\rho(f, \ell) df d\ell$  with discrete probabilities  $\rho(f_i, \ell_j)$  for each of the traits. For example, the population-level dispersal kernel for discretely structured population variation is  $\sum_j k_{\ell_j}(v) \rho_L(\ell_j)$ , where  $\rho_L(\ell_j) = \sum_i \rho(f_i, \ell_j)$  is the marginal distribution of the individual dispersal rates (Fig. 1).

### Accounting for perfect transmission of traits

To account for seeds potentially inheriting their traits from their parents, we keep track of the density of individuals of a given trait combination at a given location. Specifically, let  $n_t(x; f, \ell)$  be the density of individuals of type  $f, \ell$  at location  $x$  at time  $t$ . Let  $\nu$  be the probability of perfect inheritance. When the trait is not perfectly transmitted, we assume that it is randomly transmitted with respect to the density  $\rho(f, \ell)$ . This model of inheritance provides a simple way to tune the heritability of traits from random transmission ( $\nu = 0$ ) to perfect transmission for all individuals ( $\nu = 1$ ). From a population genetics standpoint, this model corresponds to Turelli's (1984) 'house of cards' model where mutations occur with probability  $1 - \nu$  and the traits of the mutants are randomly drawn with respect to  $\rho(f, \ell)$ .

Under these assumptions, the model becomes

$$n_{t+1}(x; f, \ell) = \int_{-\infty}^{\infty} k_{\ell}(x-y) \times D \left( \iint n_t(y; f', \ell') df' d\ell' \right) \times \left( \nu f n_t(y; f, \ell) + (1 - \nu) \rho(f, \ell) \iint f' n_t(y; f', \ell') df' d\ell' \right) dy \quad (2)$$

where  $D(\iint n_t(y; f', \ell') df' d\ell')$  is the density-dependent reduction in fecundity at location  $y$  due to the total population density  $\iint n_t(y; f', \ell') df' d\ell'$  at location  $y$ . For discretely structured traits, we can use the same model structure by replacing the double integrals  $\iint df d\ell$  and  $\iint df' d\ell'$  with a double sums  $\sum_i \sum_j$ , and replacing the infinitesimal probabilities  $\rho(f, \ell) df d\ell$  with discrete probabilities  $\rho(f_i, \ell_j)$  for each of the traits.

### Analytic methods

To compute the asymptotic rates of spatial spread in both models, we make use of the linearization conjecture (Kot et al. 1996; Neubert and Caswell 2000; Ellner and Schreiber 2012) whose assumptions are satisfied whenever the base dispersal kernel  $k_1(v)$  has exponentially bounded tails and the density  $\rho(f, \ell)$  is compactly supported, that is, there exist  $f_{\min} < f_{\max}$  and  $\ell_{\min} < \ell_{\max}$  such that  $\iint \rho(f, \ell) df d\ell = \int_{f_{\min}}^{f_{\max}} \int_{\ell_{\min}}^{\ell_{\max}} \rho(f, \ell) d\ell df = 1$ . To use the linearization conjecture for the model with random transmission, we use the transform

$$\lambda(s) = \int_{-\infty}^{\infty} \iint f e^{sv} \frac{k_1(v/\ell)}{\ell} \rho(f, \ell) df d\ell dv$$

for the combined demography and dispersal kernel at low density. The linearization conjecture asserts that the asymptotic rate of spatial spread equals

$$c^* = \min_{s > 0} \frac{\log \lambda(s)}{s} \quad (3)$$

where the minimum is taken over values of  $s$  for which  $\lambda(s)$  is well-defined. Note that equation (3) describes the spread rate on a generational time scale. To get a yearly rate of spread, we divide this generational rate of spread by the generation time in years.

For the model with perfect transmission, define the full demography and dispersal kernel  $K(f, \ell; f', \ell', v)$  by

$$K(f, \ell; f', \ell', v) = k_{\ell}(v) f \nu \delta_{(f, \ell)}(f', \ell') + (1 - \nu) \rho(f', \ell')$$

where  $\delta_{(f, \ell)}(f', \ell')$  is the Dirac delta function at  $(f, \ell)$ . Let  $H(s)$  be the operator that takes function of the form  $n(f, \ell)$  to the function

$$(Hn)(f', \ell') = \int_{-\infty}^{\infty} \left( \iint K(f, \ell; f', \ell', v) e^{sv} df d\ell \right) dv$$

and let  $\lambda(s)$  be the dominant eigenvalue of  $H(s)$ . Then, the asymptotic rate of spatial spread is, once again, given by equation (3). When the individual variation is discretely structured, these formulas still apply but the double integrals  $\iint$  need to be replaced with double sums  $\sum_i \sum_j$  and the density functions need to be replaced with probability distribution functions.

We use equation (3) in three ways. First, we approximate its solution for small variances. Namely, let  $F$  and  $L$  be random variables with joint density  $\rho(f, \ell)$ . Then, we can express these random variables in the form  $F = \bar{F} + \sigma_F^2 Z_F$  and  $L = \bar{L} + \sigma_L^2 Z_L$ , where  $\bar{F}$  and  $\sigma_F^2$  are the mean and variance of the fecundity,  $\bar{L}$  and  $\sigma_L^2$  are the mean and variance of the mean dispersal distance  $L$ , and  $Z_F = (F - \bar{F})/\sigma_F$  and  $Z_L = (L - \bar{L})/\sigma_L$  are random variables with a mean of 0 and variance of 1. In Appendix A, we derive approximations for the rates of spatial spread when  $\sigma_F^2$  and  $\sigma_L^2$  are sufficiently small. Second, to understand the effect of perfect transmission on rates of spatial spread, we use the reduction principle (Karlin 1976; Altenberg and Feldman 1987; Kirkland et al. 2006; Altenberg 2012) in Appendix B to show that the rate of spatial spread increases with the probability  $\nu$  of perfect transmission. Moreover, we derive an explicit approximation of the rate of spread for low levels of perfect transmission. While all of our analytical results apply both to continuous and discretely structured traits, we present the arguments in the Appendices for continuously structured traits. The same arguments apply to discretely structured traits by replacing integrals with sums.

Finally, we use equation (3) for our numerical calculations. The numerical calculations were based on empirical fits of dispersal data for the tree *Acer rubrum* (Clark 1998; Clark et al. 1998b). Clark et al. (1998b) collected data on seed rain over 5 years from 100 seed traps located within five 0.36-ha mapped tree stands in the southern Appalachians. When fit with a Gaussian dispersal kernel, the distance parameter  $\alpha$  equals  $30.8 \pm 3.80$  SE (average distance travelled is  $\alpha \Gamma(1)/\Gamma(1/2) = 17.4$ ). Clark (1998) estimated the net reproductive rate as 1325 and the generation time at  $T = 5.8$  years. To get yearly rates of spread, we followed Clark (1998) and used  $c/T$ . The distribution of mean dispersal rates and fecundity were drawn from a hundred samples of a log-normal distribution with the variance and correlations reported in the figures.

## Results

Let  $\bar{F}$  and  $\bar{L}$  be the mean lifetime fecundity and mean dispersal rate of the population:  $\bar{F} = \iint f\rho(f, \ell)dfd\ell$  and  $\bar{L} = \iint \ell\rho(f, \ell)dfd\ell$ . Let  $\sigma_F^2$  and  $\sigma_L^2$  be the associated variances:  $\sigma_F^2 = \iint (f - \bar{F})^2 \rho(f, \ell)dfd\ell$  and  $\sigma_L^2 = \iint (\ell - \bar{L})^2 \rho(f, \ell)dfd\ell$ . Let  $r$  be the correlation between the lifetime fecundity of individuals and the dispersal rates of their seeds:  $r = \iint (f - \bar{F})(\ell - \bar{L})\rho(f, \ell)dfd\ell / (\sigma_F\sigma_L)$ . Let  $m(s) = \int_{-\infty}^{\infty} e^{sv} k_1(v/\bar{L})/\bar{L} dv$  be the moment-generating function for the dispersal kernel of the mean dispersal phenotype.

### Individual variation in dispersal rates

Using analytical approximations for small individual variation in dispersal rates, Appendix A demonstrates that randomly transmitted variation in dispersal rates increases the rate of spatial spread by a term proportional to the squared coefficient of variation in the mean dispersal distances. Specifically, for sufficiently small variance  $\sigma_L$ , the increase is the spread rate equals

$$\frac{m''(s^*)s^*}{2m(s^*)} \times \left(\frac{\sigma_L}{\bar{L}}\right)^2. \quad (4)$$

The proportionality constant  $\frac{m''(s^*)s^*}{2m(s^*)}$  tends to increase with the variance in the base dispersal kernel; the greater this variance, the greater the increase in the rate of spread. Intuitively, if the base mode of dispersal has greater variation in distances travelled (e.g. the Laplacian kernel with a fatter tail versus the normal with a thinner tail), the greater the likelihood of individuals moving greater distances and it is these individuals that determine the rate of spatial spread.

When some of the variation in mean dispersal distances is perfectly transmitted to offspring, Appendix B shows that there always is an additional increase in the rate of spread. When the variation in dispersal rates is small and the probability of perfect transmission is small, this additional increase is proportional to the product of the coefficient of variation in the mean dispersal distance and the probability of perfect transmission. Specifically,

$$\frac{m'(s^*)^2 s^*}{m(s^*)^2} \times \left(\frac{\sigma_L}{\bar{L}}\right)^2 \times \nu. \quad (5)$$

Consistent with the analytical predictions, numerical calculations for *A. rubrum* based on equation (3) show that variation in dispersal rates and the heritability of this variation increase rates of spread (Fig. 2A). However, at higher levels of variation, the approximation overestimates the spread rates (Fig. 2B). Nonetheless, the qualitative trends of variation in dispersal rates and perfect transmission of this variation increasing rates of spread still hold. Notably, even for moderate levels of variation and perfect transmission, individual variation in dispersal rates gives substantial boosts to the predicted rate of spread for *A. rubrum*. For example, a squared coefficient of variation of 0.5 more than doubles the rate of spatial spread (from  $\sim 20$  to  $\sim 45$  m year $^{-1}$ ). If half of this variation is perfectly transmitted, then the spread rate nearly triples to 60 m year $^{-1}$ .

### Individual variation in fecundity

Randomly transmitted variation in fecundity has no effect on rates of spatial spread. However, when some of this variation is perfectly transmitted, Appendix B shows that there always is an increase in the spread rate. For low levels of individual variation in fecundity and perfect transmission, the invasion speed increases by a term proportional to the product of the squared coefficient of variation in fecundity and the probability of perfect transmission. Specifically,

$$\frac{1}{s^*} \times \left(\frac{\sigma_F}{\bar{F}}\right)^2 \times \nu. \quad (6)$$

Figure 3 illustrates these effects numerically using equation (3) for the *A. rubrum* model. In contrast to individual variation in dispersal rates, heritable variation in fecundity for this specific model has small effects on rates of spatial spread. For example, a coefficient of variation of 1 with a 50 % chance of perfect transmission, speeds only increase  $\sim 9\%$  for fecundity variation (Fig. 3A) in contrast to  $\sim 380\%$  for dispersal variation (Fig. 2A). This relative small increase in the rate of spatial spread stems from the relatively small proportionality constant  $1/s^* \approx 8$  in (6) compared to the proportionality constants in equation (4) with  $\frac{m'(s^*)^2 s^*}{2m(s^*)} \approx 900$  and equation (5) with  $\frac{m'(s^*)^2 s^*}{m(s^*)^2} \approx 1700$ .

### Co-variation in dispersal rates and fecundity

If lifetime fecundity of parents co-vary with dispersal rates of their seeds and this variation is randomly transmitted, then Appendix A shows that the spread rate increases by two terms: the amount due to dispersal variation alone in equation (4) plus an additional term proportional to the co-variance of  $L$  and  $F$ :

$$\frac{m'(s^*)}{m(s)} \times r \times \frac{\sigma_L}{\bar{L}} \times \frac{\sigma_F}{\bar{F}}. \quad (7)$$

If this co-variation is perfectly transmitted with probability  $\nu$ , then Appendix B shows that there always is an additional increase to the spread rate. For low levels of individual variation and perfect transmission, this additional increase is proportional to the product of the co-variance between fecundities and dispersal rates and the probability of perfect transmission:

$$\frac{2m'(s^*)}{m(s^*)} \times r \times \frac{\sigma_L}{\bar{L}} \times \frac{\sigma_F}{\bar{F}} \times \nu. \quad (8)$$

For the *A. rubrum* model, Fig. 4 illustrates the substantial increase due to this co-variation: high positive correlation and heritability of individual variation in fecundity and dispersal rates (red curve in Fig. 4A) can lead to an 8-fold increase in the rate of spatial spread ( $\sim 160$  m year $^{-1}$ ) compared to the  $\sim 4$ -fold increase ( $\sim 74$  m year $^{-1}$ ) due to uncorrelated variation in fecundity and dispersal rates (blue curve in Fig. 4A).

## Discussion

Dispersal and fecundity are two fundamental traits underlying the spread of populations (Fisher 1937; Skellam 1951; Kot et al. 1996; Neubert and Caswell 2000). We show that inclusion of individual variation and co-variation of these traits shifts predictions of population spread. Our results indicate that variation in dispersal increases spread rates of populations regardless of the mode of transmission, while variation in fecundity only increases spread rates when some of this variation is heritable. The highest increases in spread rates occur when variation in dispersal positively co-varies with fecundity. Spread rates generally increase as heritability of dispersal rates and fecundity increase. Although we focus on plants, our results are also applicable to animal systems.

Our results are in line with previous mathematical studies that show accelerated spread rates when individuals within the population vary in their dispersal ability (Bouin et al. 2012; Stover et al. 2014). For gamma-distributed variation in dispersal rates and uniform distributions on two dispersal rates, Stover et al. (2014) showed that the moment-generating functions of the population-level dispersal kernels increase with individual variation in dispersal rates and, thereby, increase spread rates. However, their numerical explorations found modest increases in spread rates when compared to our *A. rubrum*

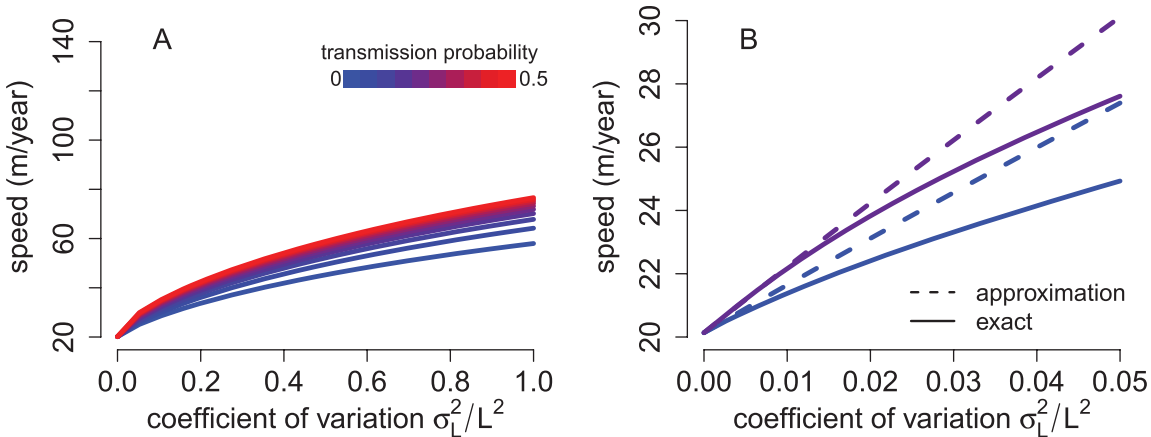


Figure 2. Individual variation in dispersal rates increases rate of spatial spread. In (A), rates of spatial spread for *Acer rubrum* (see Model and Methods) are plotted against the coefficient of variation of the dispersal rate and for increasing probabilities of perfect transmission (from blue to red). In (B), the analytical approximations (dashed lines) provide a good approximation to the exact invasion speeds (solid lines) for low variability and transmission probabilities. Higher levels of variation (A) have a decelerating effect on rates of spatial spread.

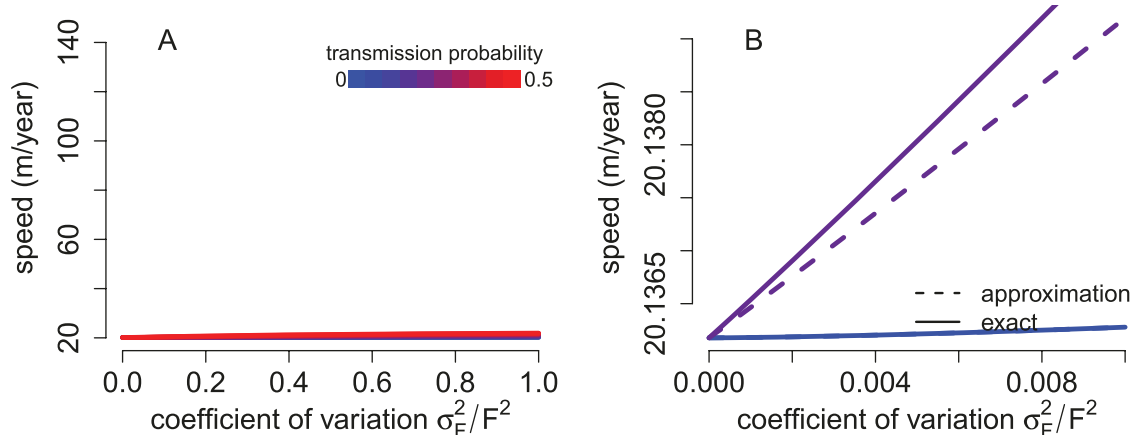


Figure 3. Individual variation in fecundity increases rate of spatial spread only when it is heritable. In (A), invasion speeds for *Acer rubrum* (see Model and Methods) are plotted against the coefficient of variation of fecundity and for increasing probabilities of perfect transmission (from blue to red). In (B), for low variability and transmission probabilities, the analytical approximations (dashed lines) provide a good approximation to the exact invasion speeds (solid lines). Higher levels of variation (A) have non-linear effects on these invasion speeds.

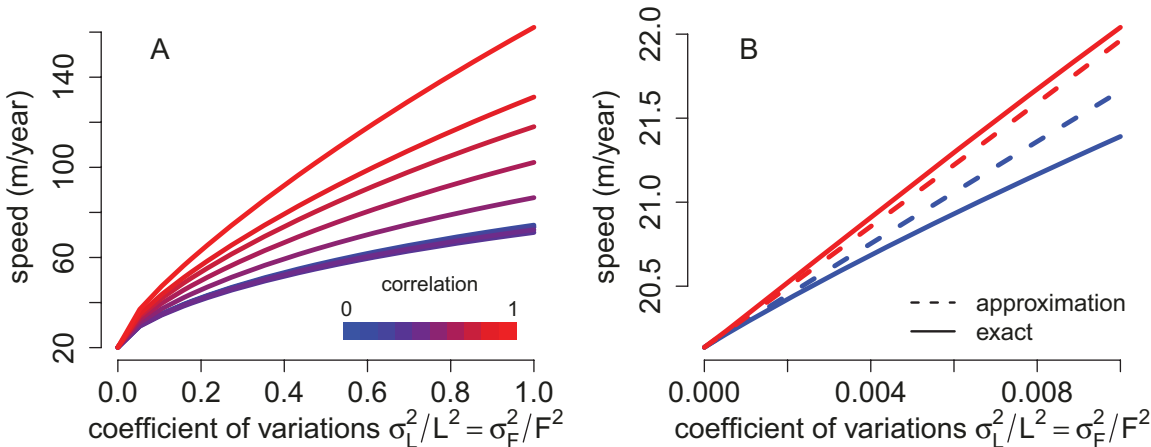


Figure 4. Co-variation in fecundity and dispersal rates leads to faster rates of spatial spread. In (A), spread rates for *Acer rubrum* (see Model and Methods) are plotted against the coefficient of variations of fecundity and dispersal rates, and for increasing correlations between fecundity and dispersal rates (from blue to red). In (B), for low variability, the analytical approximations (dashed lines) provide a good approximation to the exact invasion speeds (solid lines). Probability of perfect transmission is 0.5 in (A) and is 0.1 in (B).

example (e.g. about 20 % in (Stover *et al.* 2014, Fig. 3) versus 300 % increase in spread rates for a squared coefficient of variation of 1). Our analytic approximation (see equation (4)) highlights that this type of difference stems from differences in mean dispersal rates. Specifically, the mean dispersal rate of *A. rubrum* (30.8 m year<sup>-1</sup>) being greater than the base dispersal rate used by Stover *et al.* (2014) (1 m year<sup>-1</sup>). When intraspecific variability in dispersal rates is mostly heritable, Bouin *et al.* (2012) demonstrated that the spread rate is essentially determined by the genotypes with the highest dispersal rate being selected for at the edge of the spatial range, referred to as spatial sorting. Complementing this result, we used Karlin's reduction principle (Karlin 1976; Altenberg 2012) to show that greater heritability leads to faster spread rates. Indeed, at low levels of heritability, equation (5) implies that the increase in spread rates is constrained by the coefficient of variation in the dispersal rates and the shape of population's base dispersal kernel.

In contrast to individual variation in dispersal rates, we find that non-heritable variation in fecundity has no effect on rates of spatial spread. This outcome stems from (i) our analysis focusing on populations being sufficiently large that demographic stochasticity is negligible and (ii) the Laplace transform of the demography-dispersal kernel being a linear function of local demographic rates and a convex function of dispersal rates. As local demographic stochasticity slightly decreases spread rates (Snyder 2003; Reluga 2016) and individual variation in fecundity increases demographic stochasticity (Lloyd-Smith *et al.* 2005), it seems likely that demographic stochasticity coupled with individual variation in fecundity would decrease spread rates further. In contrast, we found that heritable variation in fecundity increases rates of spatial spread. In the extreme of this variation being perfectly transmitted from parents to offspring, we anticipate that spread rates are determined by selection for the most fecund individuals throughout the spatial range, unlike the spatial sorting mechanism for heritable variation in dispersal rates where selection only occurs at the edge of the spatial range (Bouin *et al.* 2012).

We find the biggest effects of individual variation when dispersal rates and fecundity co-vary to form dispersal syndromes within species. Specifically, positive co-variation of these traits, as has been found for some wind- and endozoochorous-dispersed seeds (reviewed in Schupp *et al.* 2019; Snell *et al.* 2019), always increases spread rates (e.g. more than doubling spread rates for *A. rubrum*). Heritability of this co-variation leads to greater increases of spatial spread. For example, our analysis implies that 50 % heritability of this co-variation can double the increase in spread rates (i.e. equations (7) and (8) are equal when  $\nu = 0.5$ ). In contrast, our analytic approximations in equations (7) and (8) imply that negative correlations between fecundity and dispersal rates lead to slower spread rates, but these rates are still higher than if there were no individual variation in fecundity or dispersal. Interestingly, Elliott and Cornell (2012) demonstrated that when there is trade-off between fecundity and dispersal (i.e. a negative correlation), polymorphisms of high- and low-fecundity individuals maintained by mutation lead to faster spread rates than the monomorphic spread rates. Whether these effects of co-variation on spread rates are operating in natural systems remains to be seen.

Here we consider the influence of variation in dispersal, variation in fecundity and their co-variation on population spread rates under several simplifying assumptions. Understanding how relaxing these assumptions may alter these predictions provide many avenues for future research. Notably, we assumed the environment is spatially and temporally

homogeneous. However, heterogeneous environments may alter these predictions. Heterogeneous environments can arise from natural disturbances, such as tree fall gaps, or through habitat loss and destruction due to human impacts. The latter tends to result in the fragmentation of the landscape into smaller, isolated fragments within a human-modified matrix. This fragmentation can alter rates of spatial spread (Shigesada *et al.* 1986; Kinezaki *et al.* 2010; Williams *et al.* 2016b; Crone *et al.* 2019). For example, Shigesada *et al.* (1986) showed that habitat fragmentation slows down and, when sufficiently severe, halts spatial spread. Alternatively, temporal variation in fecundity and dispersal rates, respectively, slow down and speed up rates of spatial spread (Ellner and Schreiber 2012). To what extent heritable or non-heritable variation in dispersal rates and fecundity counter or amplify these effects of temporal and spatial heterogeneity remains to be understood. Furthermore, it would be useful to see how individual variation due to ontogenetic changes (Ellner *et al.* 2016) or genetics beyond the 'house of cards' model (see, e.g. Johnson and Barton 2005) influences our predictions about individual variation on spatial spread.

## Conclusion

Predictions of spread tend to rely on mean estimates of population parameters for dispersal and life-history traits, but these may vary within a population and evolve through time. We found increased heritability in dispersal and fecundity increases spread rates compared to random transmission of traits, and if these are positively co-varying to form dispersal syndromes within species, selection further facilitates increased spread rates. However, if dispersal and fecundity co-vary with other life-history traits, selection for these traits may be constrained by or indirectly influence the evolution of other life-history traits, such as competitive ability or defence against natural enemies. The degree to which plant populations exhibit heritability of variation in dispersal or dispersal syndromes in which fecundity and dispersal co-vary positively is key to predicting the speed at which populations will track shifting habitats.

## Sources of Funding

This research was inspired by discussions at the (i) Seed Dispersal Workshop held in May 2016 at the Socio-Environmental Synthesis Center in Annapolis, MD, and supported by the US National Science Foundation Grant DEB-1548194 to N.G.B. and the National SocioEnvironmental Synthesis Center under the US National Science Foundation Grant DBI1052875, and (ii) the 2017 organized oral session 'Consequences of Individual Variation in Dispersal for Recruitment, Populations, and Communities' at the Annual Meetings of the Ecological Society of America in Portland, OR (organized by N.G.B., R. S. Snell, B. A. Loiselle, E. W. Schupp and E. C. Fricke). S.J.S. was supported in part by US National Science Foundation Grants DMS 1313418, 1716803.

## Contributions by the Authors

S.J.S. and N.G.B. developed the model, designed the numerical experiments, and wrote the manuscript. S.J.S. carried out the mathematical analyses and the numerical experiments.

## Conflict of Interest

None declared.

## Acknowledgements

We thank Haldre Rogers and two anonymous reviewers for suggestions that improved this paper.

## Literature Cited

Altenberg L. 2012. Resolvent positive linear operators exhibit the reduction phenomenon. *Proceedings of the National Academy of Sciences of the United States of America* 109:3705–3710.

Altenberg L, Feldman MW. 1987. Selection, generalized transmission and the evolution of modifier genes. I. The reduction principle. *Genetics* 117:559–572.

Beckman NG, Aslan CE, Rogers HS, Kogan O, Bronstein JL, Bullock JM, Hartig F, HilleRisLambers J, Zhou Y, Zurell D, Brodie JF, Bruna EM, Cantrell RS, Decker RR, Effiom E, Fricke EC, Gurski K, Hastings A, Johnson JS, Loiselle BA, Miriti MN, Neubert MG, Pejchar L, Poulsen JR, Pufal G, Razafindrakarivo OH, Sandor ME, Shea K, Schreiber S, Schupp EW, Snell RS, Strickland C, Zambrano J. 2020. Advancing an interdisciplinary framework to study seed dispersal ecology. *AoB Plants* in press.

Beckman NG, Bullock JM, Salguero-Gómez R. 2018. High dispersal ability is related to fast life history strategies. *Journal of Ecology* 106:1349–1362.

Bolnick DI, Amarasekare P, Araújo MS, Bürger R, Levine JM, Novak M, Rudolf VH, Schreiber SJ, Urban MC, Vasseur DA. 2011. Why intraspecific trait variation matters in community ecology. *Trends in Ecology & Evolution* 26:183–192.

Bonte D, Dahirel M. 2017. Dispersal: a central and independent trait in life history. *Oikos* 126:472–479.

Bouin E, Calvez V, Meunier N, Mirrahimi S, Perthame B, Raoul G, Voituriez R. 2012. Invasion fronts with variable motility: phenotype selection, spatial sorting and wave acceleration. *Comptes Rendus Mathématique* 350:761–766.

Clark JS. 1998. Why trees migrate so fast: confronting theory with dispersal biology and the paleorecord. *The American Naturalist* 152:204–224.

Clark JS, Fastie C, Hurlt G, Jackson ST, Johnson C, King GA, Lewis M, Lynch J, Pacala S, Prentice C, Schupp EW, Webb T, Wyckoff P. 1998a. Reid's paradox of rapid plant migration - dispersal theory and interpretation of paleoecological records. *Bioscience* 48:13–24.

Clark JS, Macklin E, Wood L. 1998b. Stages and spatial scales of recruitment limitation in southern Appalachian forests. *Ecological Monographs* 68:213–235.

Crone EE, Brown LM, Hodgson JA, Lutscher F, Schultz CB. 2019. Faster movement in nonhabitat matrix promotes range shifts in heterogeneous landscapes. *Ecology* 100:e02701.

Cwynar LC, MacDonald GM. 1987. Geographical variation of lodgepole pine in relation to population history. *The American Naturalist* 129:463–469.

Elliott EC, Cornell SJ. 2012. Dispersal polymorphism and the speed of biological invasions. *PLoS One* 7:e40496.

Ellner SP, Childs DZ, Rees M. 2016. *Data-driven modelling of structured populations*. Cham: Springer.

Ellner SP, Schreiber SJ. 2012. Temporally variable dispersal and demography can accelerate the spread of invading species. *Theoretical Population Biology* 82:283–298.

Fisher RA. 1937. The wave of advance of advantageous genes. *Annals of Eugenics* 7:355–369.

Hastings A, Cuddington K, Davies KF, Dugaw CJ, Elmendorf S, Freestone A, Harrison S, Holland M, Lambrinos J, Malvadkar U, Melbourne BA, Moore K, Taylor C, Thomson D. 2005. The spatial spread of invasions: new developments in theory and evidence. *Ecology Letters* 8:91–101.

Huang F, Peng S, Chen B, Liao H, Huang Q, Lin Z, Liu G. 2015. Rapid evolution of dispersal-related traits during range expansion of an invasive vine *Mikania micrantha*. *Oikos* 124:1023–1030.

Hughes CL, Dytham C, Hill JK. 2007. Modelling and analysing evolution of dispersal in populations at expanding range boundaries. *Ecological Entomology* 32:437–445.

Jindal SK, Arora D, Ghai TR. 2010. Variability studies for yield and its contributing traits in okra. *Electronic Journal of Plant Breeding* 1:1495–1499.

Johnson T, Barton N. 2005. Theoretical models of selection and mutation on quantitative traits. *Philosophical Transactions of the Royal Society of London. Series B, Biological Sciences* 360:1411–1425.

Johnson JS, Cantrell RS, Cosner C, Hartig F, Hastings A, Rogers HS, Schupp EW, Shea K, Teller BJ, Yu X, Zurell D, Pufal G. 2019. Rapid changes in seed dispersal traits may modify plant responses to global change. *AoB Plants* 11:plz020; doi:10.1093/aobpla/plz020.

Jongejans E, Skarpaas O, Shea K. 2008. Dispersal, demography and spatial population models for conservation and control management. *Perspectives in Plant Ecology Evolution and Systematics* 9:153–170.

Karlin S, ed. 1976. Population subdivision and selection migration interaction. In: *Population genetics and ecology*. New York: Academic Press, 617–657.

Kinezaki N, Kawasaki K, Shigesada N. 2010. The effect of the spatial configuration of habitat fragmentation on invasive spread. *Theoretical Population Biology* 78:298–308.

Kirkland S, Li CK, Schreiber SJ. 2006. On the evolution of dispersal in patchy landscapes. *SIAM Journal on Applied Mathematics* 66:1366–1382.

Kot M, Lewis MA, van den Driessche P. 1996. Dispersal data and the spread of invading organisms. *Ecology* 77:2027–2042.

Lloyd-Smith JO, Schreiber SJ, Kopp PE, Getz WM. 2005. Superspreading and the effect of individual variation on disease emergence. *Nature* 438:355–359.

Moran EV, Hartig F, Bell DM. 2016. Intraspecific trait variation across scales: implications for understanding global change responses. *Global Change Biology* 22:137–150.

Neubert MG, Caswell H. 2000. Demography and dispersal: calculation and sensitivity analysis of invasion speed for structured populations. *Ecology* 81:1613–1628.

Norghauer JM, Newberry DM. 2015. Tree size and fecundity influence ballistic seed dispersal of two dominant mast-fruiting species in a tropical rain forest. *Forest Ecology and Management* 338:100–113.

Norghauer JM, Nock CA, Grogan J. 2011. The importance of tree size and fecundity for wind dispersal of big-leaf mahogany. *PLoS One* 6:e17488.

Perkins TA, Phillips BL, Baskett ML, Hastings A. 2013. Evolution of dispersal and life history interact to drive accelerating spread of an invasive species. *Ecology Letters* 16:1079–1087.

Petrovskii S, Morozov A. 2008. Dispersal in a statistically structured population: fat tails revisited. *The American Naturalist* 173:278–289.

Phillips BL, Brown GP, Shine R. 2010. Life-history evolution in range-shifting populations. *Ecology* 91:1617–1627.

Phillips BL, Brown GP, Travis JM, Shine R. 2008. Reid's paradox revisited: the evolution of dispersal kernels during range expansion. *The American Naturalist* 172:S34–S48.

Reluga TC. 2016. The importance of being atomic: ecological invasions as random walks instead of waves. *Theoretical Population Biology* 112:157–169.

Ronce O, Clobert J. 2012. Dispersal syndromes, book section 10. In: Clobert J, Baguette M, Benton TG, Bullock JM, eds. *Dispersal ecology and evolution*. UK: Oxford University of Press, 119–138.

Saastamoinen M, Bocedi G, Cote J, Legrand D, Guillaume F, Wheat CW, Fronhofer EA, Garcia C, Henry R, Husby A, Baguette M, Bonte D, Coulon A, Kokko H, Matthysen E, Niitepõld K, Nonaka E, Stevens VM, Travis JMJ, Donohue K, Bullock JM, Del Mar Delgado M. 2018. Genetics of dispersal. *Biological Reviews of the Cambridge Philosophical Society* 93:574–599.

Santini L, Cornulier T, Bullock JM, Palmer SCF, White SM, Bocedi G, Rondinini C, Travis JMJ. 2016. Modelling spread rate in terrestrial mammals and the ability to track a shifting climate: a trait space approach. *Global Change Biology* 22:2415–2424.

Schupp EW, Zwolak R, Jones LR, Snell RS, Beckman NG, Aslan C, Cavazos BR, Effiom E, Fricke EC, Montaña-Centellas F, Poulsen J, Razafindrakarivo OH, Sandor ME, Shea K. 2019. Intrinsic and extrinsic drivers of intraspecific variation in seed dispersal are diverse and pervasive. *AoB Plants* 11:plz067.

Shea K, Jongejans E, Skarpaas O, Kelly D, Sheppard AW. 2010. Optimal management strategies to control local population growth or population spread may not be the same. *Ecological Applications* 20:1148–1161.

Shigesada N, Kawasaki K, Teramoto E. 1986. Traveling periodic waves in heterogeneous environments. *Theoretical Population Biology* 30:143–160.

Skellam JG. 1951. Random dispersal in theoretical populations. *Biometrika* 38:196–218.

Snell RS, Beckman NG, Fricke E, Loiselle BA, Carvalho CS, Jones LR, Lichti NI, Lustenhouwer N, Schreiber SJ, Strickland C, Sullivan LL, Cavazos BR, Giladi I, Hastings A, Holbrook KM, Jongejans E, Kogan O,

Montaño-Centellas F, Rudolph J, Rogers HS, Zwolak R, Schupp EW. 2019. Consequences of intraspecific variation in seed dispersal for plant demography, communities, evolution and global change. *AoB Plants* 11:plz016; doi:10.1093/aobpla/plz016.

Snyder RE. 2003. How demographic stochasticity can slow biological invasions. *Ecology* 84:1333–1339.

Stover JP, Kendall BE, Nisbet RM. 2014. Consequences of dispersal heterogeneity for population spread and persistence. *Bulletin of Mathematical Biology* 76:2681–2710.

Tabassum S, Leishman MR. 2018. Have your cake and eat it too: greater dispersal ability and faster germination towards range edges of an invasive plant species in eastern Australia. *Biological Invasions* 20:1199–1210.

Tabassum S, Leishman MR. 2019. It doesn't take two to tango: increased capacity for self-fertilization towards range edges of two coastal invasive plant species in eastern Australia. *Biological Invasions* 21:1–13.

Travis JM, Dytham C. 2002. Dispersal evolution during invasions. *Evolutionary Ecology Research* 4:1119–1129.

Travis JM, Harris CM, Park KJ, Bullock JM. 2011. Improving prediction and management of range expansions by combining analytical and individual-based modelling approaches. *Methods in Ecology and Evolution* 2:477–488.

Travis JM, Mustin K, Benton TG, Dytham C. 2009. Accelerating invasion rates result from the evolution of density-dependent dispersal. *Journal of Theoretical Biology* 259:151–158.

Turelli M. 1984. Heritable genetic variation via mutation-selection balance: Lerch's zeta meets the abdominal bristle. *Theoretical Population Biology* 25:138–193.

Usman MG, Rafii MY, Ismail MR, Malek MA, Abdul Latif M. 2014. Heritability and genetic advance among chili pepper genotypes for heat tolerance and morphophysiological characteristics. *The Scientific World Journal* 2014:308042.

Williams JL, Kendall BE, Levine JM. 2016a. Rapid evolution accelerates plant population spread in fragmented experimental landscapes. *Science* 353:482–485.

Williams JL, Snyder RE, Levine JM. 2016b. The influence of evolution on population spread through patchy landscapes. *The American Naturalist* 188:15–26.

## Appendix A: Derivations for the random transmission model

In this appendix derivations of the main analytic results are presented. As in the main text, let  $F$  and  $L$  be random variables with joint density function  $\rho(f, \ell)$ ; more, generally  $F$  and  $L$  can be any mixture of a discrete and continuous distribution with finite moments. Then, we can rewrite (1) as

$$n_{t+1}(x) = \int_{-\infty}^{\infty} \mathbb{E}[k_L(x-y)F]D(n_t(y))n_t(y)dy \quad (A.1)$$

and  $\lambda(s)$  from the Model and Methods in the main text can be rewritten as

$$\lambda(s) = \int_{-\infty}^{\infty} \mathbb{E}[Fk_L(v/L)] \exp(-sv)dv.$$

Provided that  $F$  and  $L$  have a finite variances, we can always write  $F = \bar{F} + \sigma_F Z_F$  and  $L = \bar{L} + \sigma_L Z_L$ , where  $Z_F, Z_L$  are random variables with mean zero and variance 1,  $\bar{F}$  and  $\bar{L}$  are the expected values of  $F$  and  $L$ , and  $\sigma_F^2$  and  $\sigma_L^2$  are the variances of  $F$  and  $L$ . Let  $r$  denote the correlation between  $F$  and  $L$ .

To derive the small variance approximations, we assume that there are positive constants  $\tau_F, \tau_L$  such that  $\sigma_F = \varepsilon \tau_F$  and  $\sigma_L = \varepsilon \tau_L$  for small  $\varepsilon > 0$ . Ellner and Schreiber (2012) showed that

$$\frac{dc^*}{d\varepsilon^k} \Big|_{\varepsilon=0} = \frac{1}{s^*} \frac{\partial^k \log \lambda}{\partial \varepsilon^k} \Big|_{\varepsilon=0} (s^*) \quad (A.2)$$

where  $s^*$  is such that  $c^* = \lambda(s^*)/s^*$  for  $\varepsilon = 0$ . By Tonelli's theorem,

$$\lambda(s) = \int_{-\infty}^{\infty} \mathbb{E}[Fk_L(v/L)] \exp(-sv)dv = \mathbb{E} \left[ \int_{-\infty}^{\infty} Fk_L(v/L) / L \exp(-sv)dv \right] = \mathbb{E}[FM(Ls)]$$

where  $M(s) = \int_{-\infty}^{\infty} k_L(v) \exp(-sv)dv$ . Differentiating with respect to  $\varepsilon$  and evaluating at zero yields

$$\begin{aligned} \frac{\partial \lambda}{\partial \varepsilon} \Big|_{\varepsilon=0} &= \frac{\partial}{\partial \varepsilon} \Big|_{\varepsilon=0} \mathbb{E}[(\bar{F} + \varepsilon \tau_F Z_F) M((\bar{L} + \varepsilon \tau_L Z_L)s)] \\ &= \mathbb{E}[\tau_F Z_F M((\bar{L} + \varepsilon \tau_L Z_L)s) + (\bar{F} + \varepsilon \tau_F Z_F) M'((\bar{L} + \varepsilon \tau_L Z_L)s) \tau_L Z_L s] \Big|_{\varepsilon=0} \\ &= \mathbb{E}[\tau_F Z_F M(\bar{L}s) + \bar{F} M'(\bar{L}s) \tau_L Z_L s] = 0 \end{aligned}$$

as  $\mathbb{E}[Z_F] = \mathbb{E}[Z_L] = 0$ . Hence, we get

$$\frac{\partial \log \lambda}{\partial \varepsilon} \Big|_{\varepsilon=0} = \frac{1}{\lambda} \frac{\partial \lambda}{\partial \varepsilon} \Big|_{\varepsilon=0} = 0. \quad (A.3)$$

Differentiating a second time with respect to  $\varepsilon$  and evaluating at zero yields

$$\frac{\partial^2 \log \lambda}{\partial \varepsilon^2} \Big|_{\varepsilon=0} = -\frac{1}{\lambda^2} \left( \frac{\partial \lambda}{\partial \varepsilon} \right)^2 \Big|_{\varepsilon=0} + \frac{1}{\lambda} \frac{\partial^2 \lambda}{\partial \varepsilon^2} \Big|_{\varepsilon=0} = \frac{1}{\lambda} \frac{\partial^2 \lambda}{\partial \varepsilon^2} \Big|_{\varepsilon=0}. \quad (A.4)$$

Computing the second derivative of  $\lambda$  yields

$$\begin{aligned} \frac{\partial^2 \lambda}{\partial \varepsilon^2} \Big|_{\varepsilon=0} &= \frac{\partial^2 \lambda}{\partial \varepsilon^2} \Big|_{\varepsilon=0} \mathbb{E}[(\bar{F} + \varepsilon \tau_F Z_F) M((\bar{L} + \varepsilon \tau_L Z_L)s)] \\ &= \frac{\partial}{\partial \varepsilon} \Big|_{\varepsilon=0} \mathbb{E}[\tau_F Z_F M((\bar{L} + \varepsilon \tau_L Z_L)s) + (\bar{F} + \varepsilon \tau_F Z_F) M'((\bar{L} + \varepsilon \tau_L Z_L)s) \tau_L Z_L s] \\ &= \mathbb{E}[2\tau_F Z_F M_1 \tau_L Z_L s + \bar{F} M_2 (\tau_L Z_L s)^2] \\ &= 2M_1 \tau_F \tau_L r s + \bar{F} M_2 \tau_L^2 (s^*)^2 \end{aligned} \quad (A.5)$$

where  $M_1 = M'(\bar{L}s^*)$  and  $M_2 = M''(\bar{L}s^*)$ . Recalling that  $\sigma_F = \varepsilon \tau_F$ ,  $\sigma_L = \varepsilon \tau_L$  and  $\lambda|_{\varepsilon=0} = \bar{F} M_0$ , where  $M_0 = M(\bar{L}s^*)$ , equations (A.2)–(A.5) give the second-order approximation

$$\begin{aligned} c^*(\varepsilon) &= c^*(0) + \frac{\varepsilon^2}{2\bar{F} M_0 s^*} (2M_1 \tau_F \tau_L r s^* + \bar{F} M_2 \tau_L^2 (s^*)^2) + O(\varepsilon^3) \\ &= c^*(0) + \frac{M_1}{\bar{F} M_0} \sigma_F \sigma_L r + \frac{M_2 s^*}{2M_0} \sigma_L^2 + O(\varepsilon^3). \end{aligned} \quad (A.6)$$

Defining  $m(s) = \int_{-\infty}^{\infty} k_L(v/\bar{L}) / \bar{L} e^{vs} ds = M(\bar{L}s)$ , we get  $m'(s) = M'(\bar{L}s) \bar{L}$  and  $m''(s) = M''(\bar{L}s) \bar{L}^2$ . Hence,  $M_0 = m(s^*)$ ,  $M_1 = m(s^*)/\bar{L}$  and  $M_2 = m''(s^*)/\bar{L}^2$  and

$$c^*(\varepsilon) = c^*(0) + \frac{m'(s^*)}{m(s^*)} \frac{\sigma_F \sigma_L}{\bar{F} \bar{L}} r + \frac{m''(s^*) s^*}{2m(s^*)} \left( \frac{\sigma_L}{\bar{L}} \right)^2 + O(\varepsilon^3) \quad (A.7)$$

which gives equations (4) and (7) from the main text.

## Appendix B: Rates of spread for the model with perfect transmission

For the model with perfect transmission, recall that we have the demographic-dispersal kernel  $K_\nu(f, \ell; f', \ell', v)$  (now parameterized by  $v$ ) given by

$$K_\nu(f, \ell; f', \ell', v) = k_\ell(v) f(\nu \delta_{(f, \ell)}(f', \ell') + (1 - \nu) \rho(f', \ell')) \quad (B.1)$$

where  $\delta_{(f, \ell)}(f', \ell')$  is the Dirac delta function based at the point  $(f, \ell)$ . Let  $H_\nu(s)$  be the operator that takes the function  $n(f, \ell)$  to the function

$$(H_\nu(s)n)(f', \ell') = \int_{-\infty}^{\infty} \left( \iint K_\nu(f, \ell; f', \ell', v) e^{sv} n(f, \ell) df d\ell \right) dv \quad (B.2)$$

and let  $\lambda_\nu(s)$  be the dominant eigenvalue of  $H(s)$ . The rate of spatial spread, as a function of  $\nu$ , is given by  $c_\nu^* = \min_{s>0} \lambda_\nu(s)/s$ . Let  $s^*$  be the value of  $s$  that gives the rate of spread for  $\nu = 0$ , i.e. only random transmission.

Ellner and Schreiber (2012) showed that

$$\frac{dc_\nu^*}{d\nu} = \frac{1}{s^*} \frac{\partial \log \lambda_\nu}{\partial \nu}(s^*) = \frac{1}{\lambda_0 s^*} \frac{\partial \lambda_\nu}{\partial \nu}(s^*). \quad (\text{B.3})$$

We will use the reduction principle (Karlin 1976; Kirkland et al. 2006; Altenberg 2012) to show that this derivative is always positive, i.e. the rate of spatial spread increases with  $\nu$ . Then, we will compute this derivative at  $\nu = 0$  to get an approximation of the rate of spatial spread when  $\nu$  is small.

We will show that the operator  $H_\nu(s)$  can be written in the form  $(\nu \text{Id} + (1 - \nu)P)D$ , where  $\text{Id}$  is the identity operator,  $P$  is a stochastic, positive operator and  $D$  is a non-scalar multiplication operator. For operators of this form, Altenberg (2012, Theorem 6) proved that the dominant eigenvalue  $\lambda_\nu(s)$  is an increasing function of  $\nu$ . Equivalently,  $\lambda_\nu(s)$  is a decreasing function of the probability  $1 - \nu$  of mutation, i.e. the reduction principle. Using the definition of  $H_\nu(s)$  and  $K_\nu$  we have

$$\begin{aligned} (H_\nu(s)n)(f', \ell') &= \int_{-\infty}^{\infty} \left( \iint K_\ell(v) f(v\delta_{(f, \ell)}(f', \ell') + (1 - \nu)\rho(f', \ell')) e^{sv} n(f, \ell) df d\ell \right) dv \\ &= \iint M(\ell s) f(v\delta_{(f, \ell)}(f', \ell') + (1 - \nu)\rho(f', \ell')) n(f, \ell) df d\ell \\ &= v M(\ell' s) f'(n(f', \ell') + (1 - \nu)\rho(f', \ell')) \iint M(\ell s) f n(f, \ell) df d\ell \\ &= ((\nu \text{Id} + (1 - \nu)P)D)n(f', \ell') \end{aligned}$$

where  $P$  is the positive operator defined by  $(Pn)(f', \ell') = \rho(f', \ell') \iint n(f, \ell) df d\ell$  and  $D$  is the multiplication operator defined by  $(Dn)(f', \ell') = M(\ell' s) f'(n(\ell', f'))$ . Hence, by the reduction principle  $\lambda_\nu(s)$  is an increasing function of  $\nu$ . Equation (B.3) implies that  $c_\nu^*$  is an increasing function of  $\nu$ .

To find the derivative in (B.3) at  $\nu = 0$ , we need to find the dominant, left and right eigenfunctions of  $H_0(s^*)$ . The dominant, right eigenfunction  $w$  and eigenvalue  $\lambda_0$  must satisfy

$$\begin{aligned} \lambda_0 w(f', \ell') &= \int_{-\infty}^{\infty} \iint K_\ell(v) f \rho(f, \ell; f', \ell') w(f, \ell) e^{sv} df d\ell dv \\ &= \iint \left( \int_{-\infty}^{\infty} K_\ell(v) e^{sv} dv \right) f \rho(f', \ell') w(f, \ell) df d\ell \\ &= \iint M(\ell s^*) f \rho(f', \ell') w(f, \ell) df d\ell \\ &= \rho(f', \ell') \iint M(\ell s^*) f w(f, \ell) df d\ell \end{aligned}$$

Hence, we get the unique, normalized eigenfunction is  $w(f, \ell) = \rho(f, \ell)$  and eigenvalue is  $\lambda_0 = \iint M(\ell s^*) f \rho(f, \ell) df d\ell = \mathbb{E}[\text{FM}(Ls^*)]$ , where  $(F, L)$  is the random vector with density function  $\rho(f, \ell)$ . The dominant, left eigenfunction  $u(f, \ell)$  must satisfy

$$\lambda_0 u(f, \ell) = \text{fM}(\ell s^*) \iint u(f', \ell') \rho(f', \ell') df' d\ell'$$

and therefore can be chosen to equal  $u(f, \ell) = \text{fM}(\ell s^*)$ . Hence, we get

$$\frac{\partial \lambda_\nu}{\partial \nu} \Big|_{\nu=0}(s^*) = \frac{\iint u(f, \ell) (Gw)(f, \ell) df d\ell}{\iint u(f, \ell) w(f, \ell) df d\ell}$$

where  $G$  is the perturbation operator on functions  $n(f, \ell)$  defined by

$$(Gn)(f', \ell') = \int_{-\infty}^{\infty} \iint f(\delta_{f', \ell'}(f, \ell) - \rho(f', \ell')) n(f, \ell) e^{-s^* v} k_\ell(v) df d\ell dv.$$

We have

$$\iint u(f, \ell) w(f, \ell) df d\ell = \iint f \text{M}(\ell s^*) \rho(f, \ell) df d\ell = \mathbb{E}[\text{FM}(Ls^*)] = \lambda_0.$$

Furthermore,

$$\begin{aligned} \iint u(f, \ell) (Gw)(f, \ell) df d\ell &= \iint u(f, \ell) (f \text{M}(\ell s^*) \rho(f, \ell) - \rho(f, \ell) \lambda_0) df d\ell \\ &= \iint f \text{M}(\ell s^*) (f \text{M}(\ell s^*) \rho(f, \ell) - \rho(f, \ell) \mathbb{E}[\text{FM}(Ls^*)]) df d\ell \\ &= \iint (f \text{M}(\ell s^*))^2 \rho(f, \ell) df d\ell - \mathbb{E}[\text{FM}(Ls^*)]^2 \\ &= \mathbb{E}[(\text{FM}(Ls^*))^2] - \mathbb{E}[\text{FM}(Ls^*)]^2 = \text{Var}[\text{FM}(Ls^*)]. \end{aligned}$$

Thus, we get

$$\frac{dc_\nu^*}{d\nu} \Big|_{\nu=0} = \frac{1}{\lambda_0 s^*} \frac{\text{Var}[\text{FM}(Ls^*)]}{\mathbb{E}[\text{FM}(Ls^*)]} \quad (\text{B.4})$$

As in Appendix A, let  $F = \bar{F} + \sigma_F Z_F$  and  $L = \bar{L} + \sigma_L Z_L$ , where  $Z_F, Z_L$  are random variables with mean zero and variance 1,  $\bar{F}$  and  $\bar{L}$  are the expected values of  $F$  and  $L$ , and  $\sigma_F^2$  and  $\sigma_L^2$  are the variances of  $F$  and  $L$ . Let  $r$  denote the correlation between  $F$  and  $L$ . To derive the small variance approximations, we assume that there are positive constants  $\tau_F, \tau_L$  such that  $\sigma_F = \varepsilon \tau_F$  and  $\sigma_L = \varepsilon \tau_L$  for small  $\varepsilon > 0$ . With these assumptions, to get an approximation of  $\text{Var}[\text{FM}(Ls^*)]$  for small  $\varepsilon$ , we need the following three approximations

$$\begin{aligned} \mathbb{E}[\text{FM}(Ls^*)] &= \mathbb{E}[(\bar{F} + \sigma_F Z_F)(M_0 + M_1 \sigma_L Z_L s^* + M_2 (\sigma_L Z_L s^*)^2/2)] + O(\varepsilon^3) \\ &= \bar{F}(M_0 + M_2 (\sigma_L s^*)^2/2) + M_1 \sigma_F \sigma_L r s^* + O(\varepsilon^3) \end{aligned} \quad (\text{B.5})$$

where  $M_0 = M(\bar{L}s^*)$ ,  $M_1 = M'(\bar{L}s^*)$  and  $M_2 = M''(\bar{L}s^*)$ , and

$$\mathbb{E}[\text{FM}(Ls^*)]^2 = (\bar{F}M_0)^2 + \bar{F}^2 M_0 M_2 (\sigma_L s^*)^2 + 2\bar{F}M_0 M_1 \sigma_F \sigma_L r s^* + O(\varepsilon^3), \quad (\text{B.6})$$

and

$$\begin{aligned} \mathbb{E}[(\text{FM}(Ls^*))^2] &= \mathbb{E}[((\bar{F} + \sigma_F Z_F)(M_0 + M_1 \sigma_L Z_L s^* + M_2 (\sigma_L Z_L s^*)^2/2)^2) + O(\varepsilon^3)] \\ &= \mathbb{E}[(\bar{F}M_0 + \bar{F}M_1 \sigma_L Z_L s^* + \bar{F}M_2 (\sigma_L Z_L s^*)^2/2 + \sigma_F Z_F M_0 + \sigma_F Z_F M_1 \sigma_L Z_L s^*)^2] + O(\varepsilon^3) \\ &= (\bar{F}M_0)^2 + \bar{F}M_0 \bar{F}M_2 (\sigma_L s^*)^2 + 2\bar{F}M_0 M_1 \sigma_L \sigma_F r s^* + (\bar{F}M_1 \sigma_L s^*)^2 \\ &\quad + 2\bar{F}M_0 M_1 \sigma_L \sigma_F r s^* + M_0^2 \sigma_F^2 + O(\varepsilon^3). \end{aligned} \quad (\text{B.7})$$

Taking the difference between (B.7) and (B.6) gives us

$$\text{Var}[\text{FM}(Ls^*)] = (\bar{F}M_1 \sigma_L s^*)^2 + 2\bar{F}M_0 M_1 \sigma_L \sigma_F r s^* + M_0^2 \sigma_F^2 + O(\varepsilon^3). \quad (\text{B.8})$$

Thus, for sufficiently small  $\nu$  and  $\varepsilon$ , equation (B.4) and  $\lambda_0 = \bar{F}M_0$  implies that

$$\begin{aligned} c_\nu^* &\approx c^* + \frac{\nu}{\bar{F}M_0 s^*} \frac{(\bar{F}M_1 \sigma_L s^*)^2 + 2\bar{F}M_0 M_1 \sigma_L \sigma_F r s^* + M_0^2 \sigma_F^2}{\bar{F}M_0} \\ &= c^* + \nu \left( \frac{M_1^2 s^*}{M_0^2} \sigma_L^2 + \frac{2M_1}{\bar{F}M_0} \sigma_L \sigma_F r + \frac{1}{\bar{F}^2 s^*} \sigma_F^2 \right). \end{aligned} \quad (\text{B.9})$$

Defining  $m(s) = \int_{-\infty}^{\infty} k_1(v/\bar{L}) \bar{L} e^{vs} ds = M(\bar{L}s)$ , we get  $m'(s) = M'(\bar{L})\bar{L}$  and  $m''(s) = M''(\bar{L})\bar{L}^2$ . Hence,  $M_0 = m(s^*)$ ,  $M_1 = m'(s^*)/\bar{L}$  and  $M_2 = m''(s^*)/\bar{L}^2$  and

$$c_\nu^* \approx c^* + \nu \left( \frac{m_1(s^*)^2 s^*}{m(s^*)^2} \frac{\sigma_F^2}{\bar{L}^2} + \frac{2m_1(s^*)}{\bar{L}} \frac{\sigma_L \sigma_F}{\bar{F}} r + \frac{1}{s^*} \left( \frac{\sigma_F}{\bar{F}} \right)^2 \right) \quad (\text{B.10})$$

which gives equations (5), (6) and (8) from the main text.

We conclude by noting that provided they are bounded, all of the arguments here also apply when the joint distribution of  $F$  and  $L$  is any mixture of continuous and discrete distributions.